International Journal of Technology 14(7) 1605-1614 (2023)
Received July 2023 / Revised September 2023 / Accepted October 2023

International Journal of Technology

http://ijtech.eng.ui.ac.id

Effect of Coagulation Bath Composition on Cellulose-Based Polymer Electrolyte Fabricated via Non-Solvent-Induced Phase Separation Method

Christin Rina Ratri[1,2], Tegar Budi Aguta[1], Annisaa Hayya Arundati[3], Rohib Rohib[4], Mochamad Chalid[1], Sotya Astutiningsih[1], Adam Febriyanto Nugraha[1*]

[1]*Green Polymer Technology Laboratory, Department of Metallurgical and Materials Engineering, Faculty of Engineering, Universitas Indonesia, Depok, Jawa Barat, 16424, Indonesia*
[2]*Research Center for Advanced Materials, National Research and Innovation Agency, KST BJ Habibie Gd. 440-441, Tangerang Selatan, Banten, 15314, Indonesia*
[3]*Graduate Institute of Ferrous and Energy Materials Technology, Pohang University of Science and Technology, Pohang 37673, Republic of Korea*
[4]*Institut De Recherches Sur La Catalyse Et L'environnement De Lyon, Umr 5256, Cnrs Avenue Albert Einstein, 69626, Lyon, France*

Abstract. Cellulose acetate (CA) membrane was developed through a non-solvent-induced phase separation (NIPS) technique to replace the commercial petroleum-based Celgard separator membrane in Li-ion battery (LIB). The morphology of a membrane can have a substantial impact on both its mechanical and electrochemical properties, which are influenced by the solvent-nonsolvent interaction. Therefore, this study examined the effect of solvent fraction in an acetone-water system on the membrane morphology. CA dissolved in acetone was cast on a glass plate and immersed in the coagulation bath with varying acetone-water ratios. The resulting free-standing membrane was analyzed subsequently and showed increased porosity, hydrophilicity, and electrolyte uptake with higher acetone ratios in the coagulation bath. It was also found that a more porous membrane contributes to a lower tensile strength, including, 6.8 MPa, 5.5 MPa, 4.6 MPa, and 2.6 MPa for the coagulation baths containing 0%, 25%, 50%, and 75% acetone, respectively. These results showed that the mechanical properties of CA membranes are higher than those of commercial Celgard membranes (1.42 MPa). LIB separator performance was measured using electrochemical impedance spectroscopy (EIS). CA membrane fabricated with 50% acetone content in the coagulation bath possessed the highest ionic conductivity, 4.79×10^{-4} S/cm, which is higher than the ionic conductivity of the Celgard membrane (9.41×10^{-7} S/cm). Considering their superior mechanical properties and electrical performance, CA membranes could potentially substitute Celgard as a more sustainable alternative for LIB separators.

Keywords: Cellulose acetate; Coagulation bath; LIB separator; NIPS

1. Introduction

The increasing demand for mobile devices and electric or hybrid vehicles has led to the widespread use of lithium-ion batteries (LIBs). Their popularity is attributed to outstanding energy density, substantial specific capacity, relatively low self-discharge rate, durability, and lightweight design (Tabani, Maghsoudi, and Fathollahi Zonouz, 2021). The important

*Corresponding author's email: adam.febriyanto04@ui.ac.id, Tel.: +62-21-786-3510; Fax.: +62-21-787-2350
doi: 10.14716/ijtech.v14i7.6677

role of LIBs separators includes preventing short circuits between the electrodes and second, to absorb and optimize lithium-ion conductivity by absorbing and retaining electrolytes (Yang *et al.*, 2022).

Polyolefin separators, such as polyethylene (PE) and polypropylene (PP) membranes, are widely used due to their suitably sized pores, excellent mechanical strength, and chemical stability (Setiaji *et al.*, 2022; Razalli *et al.*, 2015). However, their primary disadvantage is insufficient liquid electrolyte capacity and the inability to absorb high-dielectric-constant electrolytes on their hydrophobic surfaces (Xu *et al.*, 2017).

To address these challenges, biodegradable battery separators, made from renewable natural-resource-based polymers, are being developed as a sustainable, non-toxic, and biodegradable alternative to petroleum-based membranes. Among these solutions, cellulose acetate (CA) is a promising host polymer for LIBs separators (Febriasari *et al.*, 2021). Subsequently, CA polymers, characterized by carbonyl and hydroxyl groups, exhibit a strong affinity for electrolytes and superior compatibility with electrodes. CA's versatility extends to film formation and efficient electrical insulation, rendering it well-suited for use as a matrix in LIBs (Li *et al.*, 2017).

Polymeric membranes can be produced in various ways including nonsolvent-induced phase separation (NIPS), thermally induced phase separation (TIPS), melt extrusion, electrospinning, and track etching (Rochardjo *et al.*, 2021). The easy processing and high reliability of NIPS membranes make them attractive choices. As a widely used method for fabricating membranes made from polymers, NIPS has several advantages over other methods. Subsequently, with NIPS, this approach facilitates fine control and generates small, evenly distributed micropores (Choi, Ingole, and Park, 2022). Furthermore, this method is superior to alternative methods, such as dry spinning and hot drawing, in terms of achieving appropriate tensile strength, biaxial strength, and puncture resistance (Kahrs and Schwellenbach, 2020; Li *et al.*, 2017). In the NIPS process, the polymer and solvent are homogeneously dissolved, poured onto a glass plate, and submerged in a nonsolvent bath (Li *et al.*, 2008). After phase separation and removal of residual solvent, the nonsolvent must have a high affinity for the solvent but not for the polymer (Wang *et al.*, 2019).

Previous NIPS studies used various approaches to fabricate porous membranes, such as changing the composition of the coagulation bath (Thankamony *et al.*, 2018). The properties and morphology of membranes are significantly influenced by the bath composition during immersion in the coagulation bath (Pagliero *et al.*, 2020). The porous membrane structure was affected by the solvent fraction in the coagulation bath (Asghar *et al.* 2018). The results showed that increasing the solvent concentration in the coagulation bath increased membrane crystallinity (Jung *et al.*, 2016).

This study specifically focuses on the preparation of CA membranes using the NIPS method. There is a gap in study addressing the contribution of solvent fractions in acetone-water systems to the effectiveness of CA-based membranes as LIB separators. In the NIPS method, the solvent amount in the coagulation bath plays a crucial role in the demixing process, influencing pore formation and potentially affecting the electrochemical performance of the membrane. Using a facile approach, a porous CA membrane with superior ionic conductivity was successfully produced for use as a lithium-ion battery separator.

2. Methods

To prepare the separators through NIPS, CA (Mn = 30,000) was dissolved in acetone until homogeneous. The dissolution process occurred at room temperature, using a vial and a magnetic stirrer (IKA C-MAG HS 7) to maintain constant stirring. After achieving

homogeneity, the solution was set aside for a period to eliminate any gas bubbles and was subsequently placed on a glass plate at room temperature.

A 15-minute evaporation process was used to partially evaporate the polymer solution. Subsequently, the glass plate was placed in a room-temperature water coagulation bath for 15 min and the membrane was peeled off slowly. Three variations of porous membranes were prepared, each based on the solvent fraction used in the coagulation bath, as shown in Table 1. The membrane was dried on sandwich-like filter paper using a vacuum desiccator for further analysis. An overview of the NIPS procedure is shown in Figure 1.

Table 1 Sample specification for the membrane fabrication

Sample code	Water/acetone (v/v)
A0W100	100/0
A25W75	75/25
A50W50	50/50
A75W25	25/75

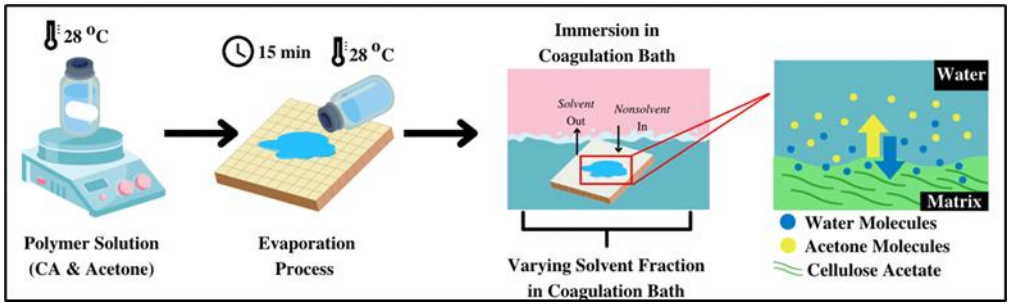

Figure 1 Overview process of the NIPS method

2.2. Cellulose Acetate Membrane Characterization

Fourier transform infrared (FTIR, Thermo Scientific iS-10 Spectra) spectroscopy was used to evaluate the functional groups of CA membrane at 4000–400 cm^{-1} absorbance under ambient conditions.

To evaluate thermal stability, changes in membrane dimensions were calculated. Approximately 2 cm diameter pieces were cut from the samples. After a 2-hour storage at 90°C, the membrane was examined for heat-induced shrinkage caused by heat. Based on Equation (1), the shrinkage was calculated (Liang *et al.*, 2018):

$$\text{Shrinkage } (\%) = \frac{(S_0 - S)}{S_0} \times 100\% \quad (1)$$

where S_o is the membrane surface area before heating and S is the membrane surface area after heating.

The contact angle was determined using the sessile drop method, using wet agents such as water, ethylene glycol, and an electrolyte (0.67 M $LiClO_4$). Using a desiccator vacuum overnight, residual humidity was removed from the membrane before the wettability test. After dropping the electrolyte solution for 3 and 30 s, the contact angles were measured.

To measure separator porosity (P), a gravimetric method based on n-butanol absorption was used. Each sample measured approximately 2 cm in diameter. Equation (2) was used to calculate the porosity of the separator (Cui *et al.*, 2017).

$$P\ (\%) = \frac{(M_n - M_i)}{\rho_n \times s \times d} \times 100\% \quad (2)$$

where P is the separator porosity, the mass of the separator at the start is M_i; the mass after an hour of n-butanol soaking is M_n, the density of n-butanol is ρ_n (0.81 g/cm^3), the separator surface area is s, and its thickness is d.

The surface and cross-section of the separator were observed using a scanning electron microscope (SEM, Hitachi SU3500, Tokyo, Japan) with an acceleration voltage of 10 kV. After analyzing the surface images, the ImageJ software was used to determine the pore sizes.

The tensile properties of the membranes were determined using a universal testing machine (UTM, Shimadzu AGS-X Series 5 kN) in accordance with ASTM D1708. The test was conducted under ambient conditions at a speed of 0.25 mm/min.

A gravimetric measurement of membrane electrolyte uptake was conducted by weighing the membranes before and after soaking in 0.67 M $LiClO_4$ for 2 h. Electrolyte uptake was measured following Equation (3).

$$\text{Electrolyte uptake} = \frac{(W_2 - W_1)}{W_1} \times 100\ \% \quad (3)$$

where W_1 shows the separator weight before and W_2 shows the weight after electrolyte soaking. The mean and standard deviation were calculated from three measurements.

Electrochemical impedance spectroscopy (EIS, Metrohm Autolab, Potentiostat Mode) was performed at frequencies ranging from 1 Hz to 1 MHz to quantify the membrane ionic conductivity between the stainless-steel electrodes. Cell assembly started with the membranes being soaked in 0.67 M $LiClO_4$ electrolyte solution for two hours before assembly. Coin cells (CR2032) were assembled using a separator and blocking electrodes. Equation (4) was used to calculate the ionic conductivity, σ (Luiso *et al.*, 2021).

$$\sigma = \frac{t}{R_b \times A} \quad (4)$$

where t is the membrane thickness, R_b is the bulk resistance, and A is the contact area between the separator and electrodes.

3. Results and Discussion

The coagulation process plays a crucial role in the formation of hollow membranes, influenced by both thermodynamics and kinetics. Membrane morphology is impacted by factors such as polymer-solvent interactions, solution viscosity, and solvent diffusivity. Typically, water serves as the most common nonsolvent. The addition of a solvent can delay instant demixing by lowering polymer concentration and decreasing nonsolvent activity. This delay in liquid-liquid demixing is the predominant effect, as this method is used to produce dense membranes (Cui *et al.*, 2017).

The identification of functional groups in CA membrane was based on FTIR spectra, analyzing the location and intensity of spectral peaks. In Figure 2, the FTIR spectrum of CA membrane shows two characteristic peaks at wavelengths of 1730 and 1220 cm^{-1}, corresponding to the C=O and C–O–C functional groups, respectively (Ramesh, Shanti, and Morris, 2013). The stretching vibration of hydroxyl group O-H was denoted by the peak at 3497 cm^{-1}, and methyl group C-H stretching at 2945 cm^{-1} (Sudiarti *et al.*, 2017), confirming the formation of true CA. Figure 2 shows the FT-IR spectra of CA in the powder and membrane forms.

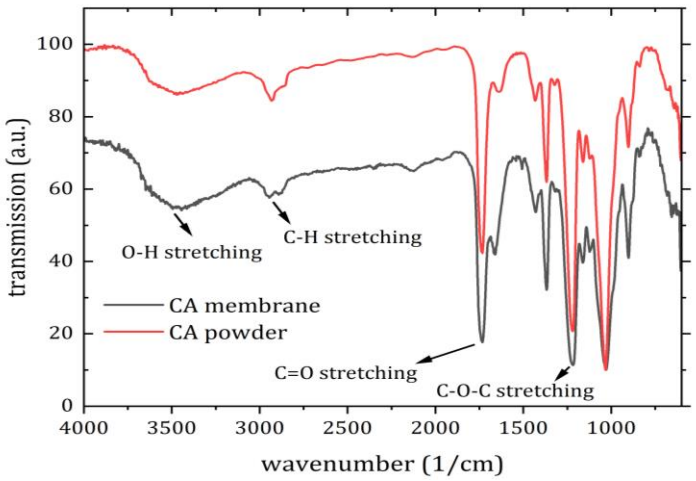

Figure 2 FT-IR spectra of cellulose acetate powder and membrane form

Porosity is a crucial factor for separators because it impedes the penetration of active components and prevents dendritic Li penetration (Ngamaroonchote and Chotsuwan 2016). The membrane obtained using the NIPS process exhibited a more porous structure compared to the solution casting method. This is showed by the SEM results shown in Figure 3.

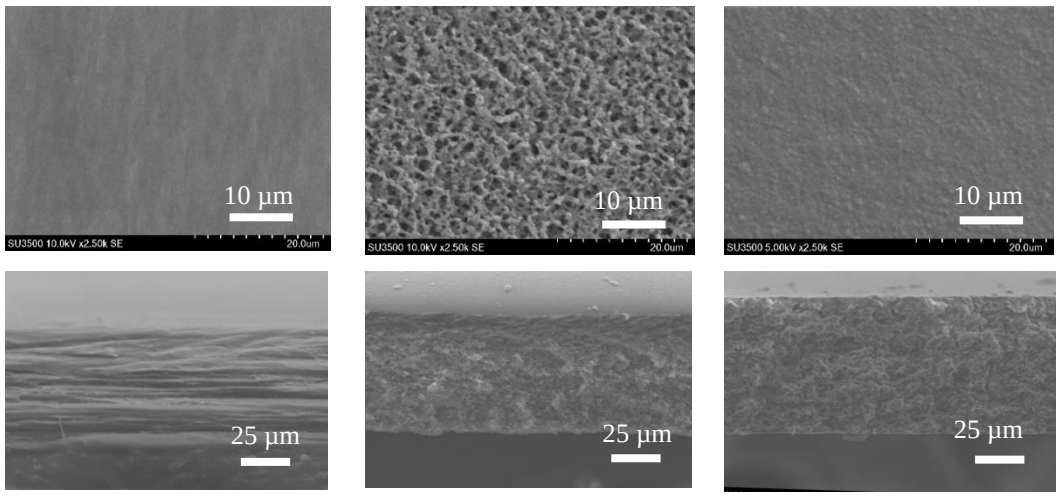

(a) (b) (c)

Figure 3 SEM micrograph of (top row) surface and (bottom row) cross-sectional morphology of (a) Celgard and cellulose acetate membrane obtained with (b) NIPS and (c) solution casting

The observation in Figure 4 shows that an increase in acetone content in the coagulation bath leads to higher porosity in CA separator. This effect is attributed to the higher acetone concentration reducing the solubility difference between the solvent and nonsolvent. This reduction promotes demixing during the coagulation process, ultimately yielding a membrane with increased porosity.

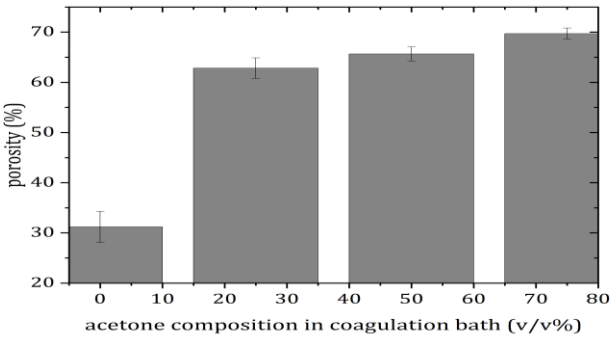

Figure 4 Influence of solvent fraction on porosity of the membrane

In LIB, specifically those with high power and energy, dimensional stability is crucial for separators. The separator should not shrink or wrinkle significantly when the temperature increases and it should minimize the thermal shrinkage during drying. As shown in Figure 5, the Thermal Shrinkage Ratio (TSR) for each composition of the coagulation bath was less than 5%. This satisfies the dimensional stability requirements of battery separator applications.

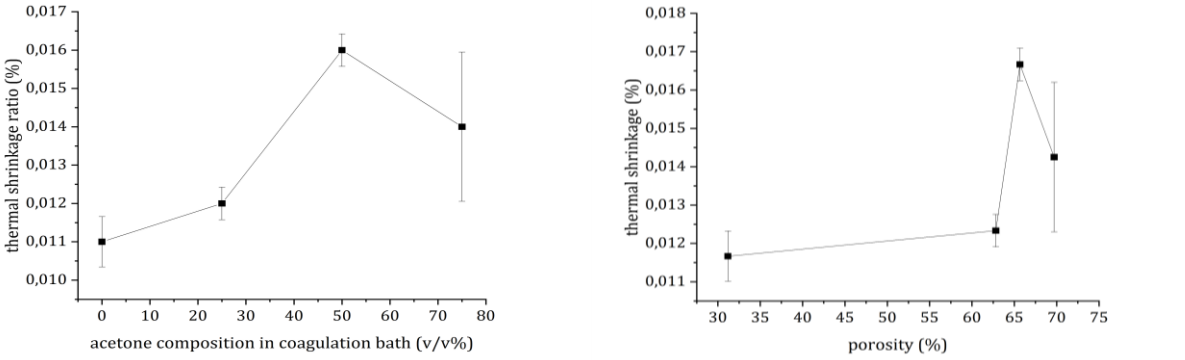

(a) (b)

Figure 5 Influence of (a) solvent fraction and (b) porosity to thermal shrinkage ratio

Membrane hydrophilicity plays a significant role in interfacial interactions and can be modified by adjusting the phase-inversion process conditions. Valuable information is obtained by measuring the contact angle between the wetting agent and the membrane surface (Song, Birbach, and Hinestroza, 2012). The results are shown in Figure 6. Increasing hydrophilicity was also observed with higher acetone composition in the coagulation bath, and this is attributed to the increasing miscibility, which accelerates the precipitation process and promotes pore formation (Silva, Belmonte-Reche, and Amorim, 2021).

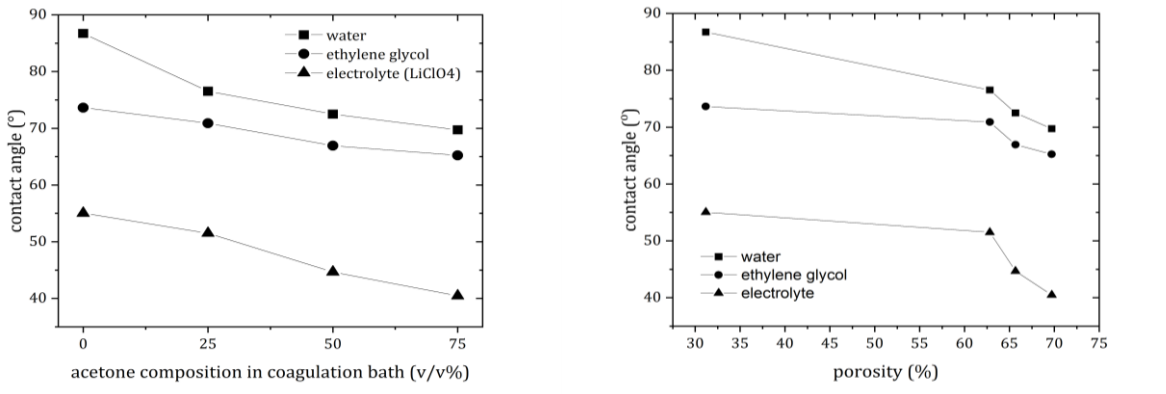

(a) (b)

Figure 6 Influence of (a) solvent fraction and (b) porosity to the membrane wettability

Figure 7 shows the influence of the solvent fraction and porosity on the membrane tensile strength. These results show that the tensile strength of CA membrane decreased with increasing acetone content in the coagulation bath. This is in accordance with the literature, as an increase in the composition of acetone causes an increase in porosity, and negatively affects the tensile strength of the membrane (Kartha and Mallik, 2020; Zhao *et al.*, 2008). The tensile strength of the Celgard membrane was measured at 1.42 MPa. All the fabricated CA separator membranes had a tensile strength that exceeded that of a conventional Celgard separator membrane.

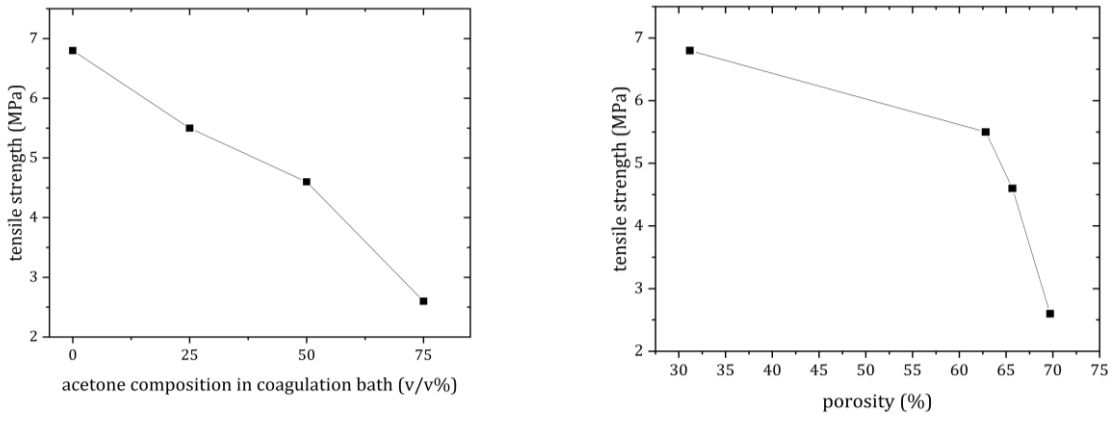

(a) (b)

Figure 7 Influence of (a) solvent fraction and (b) porosity to the tensile strength

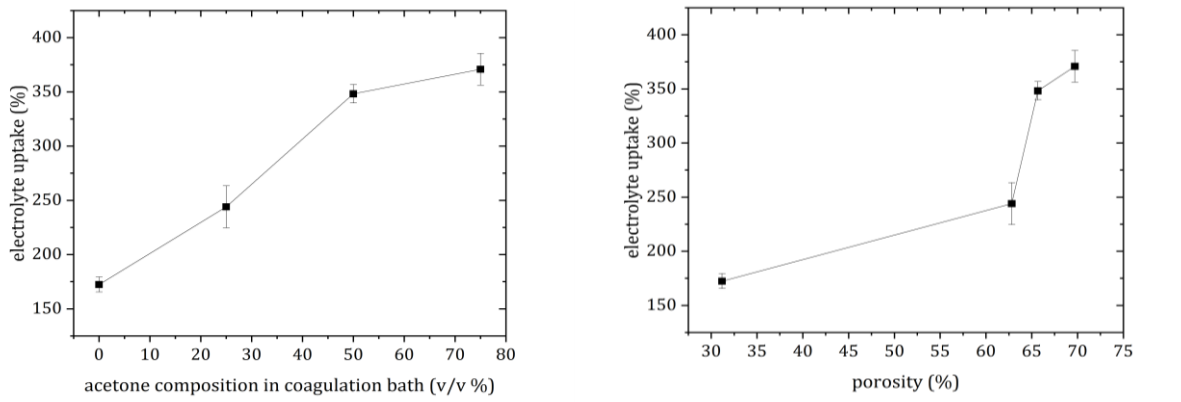

(a) (b)

Figure 8 Influence of (a) solvent fraction and (b) porosity to the electrolyte uptake

As shown in Figure 8, a higher acetone ratio in the coagulation bath resulted in a higher electrolyte uptake. This is caused by higher absorption of the electrolyte in the membrane. It is important to note that electrolyte uptake increases linearly, while the porosity increases logarithmically (Shi *et al.*, 2015). An excellent ionic conductivity is required for the separator because it controls ions passing between the positive and negative terminals (Arrieta, Barrera, and Mendoza, 2022). Subsequently, EIS measurements were performed by applying a frequency within a certain range, resulting in real and imaginary impedances presented in the Nyquist plot (Figure 9). The calculated ionic conductivities are listed in Table 2.

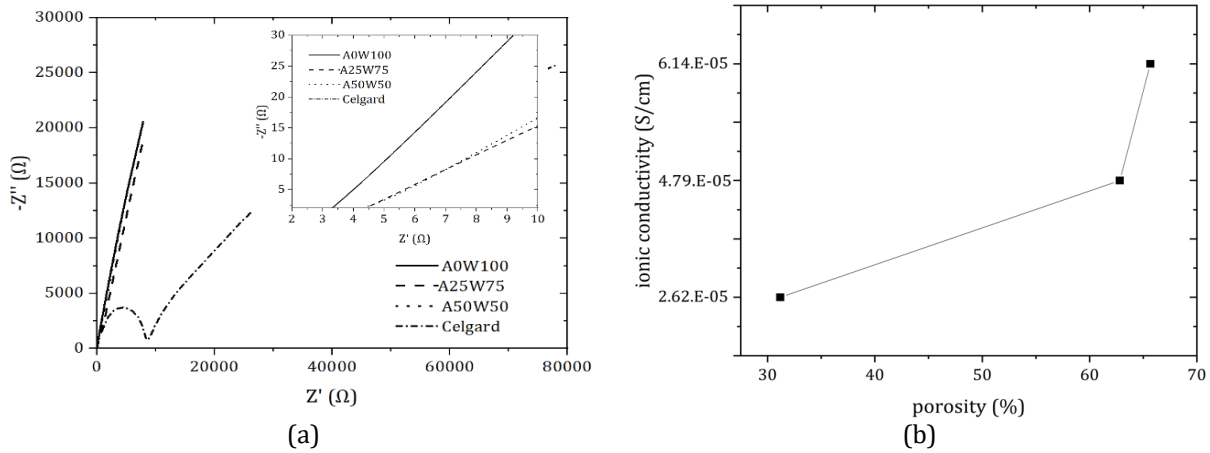

(a) (b)

Figure 9 (a) Nyquist plot of cellulose acetate membranes and (b) influence of porosity on ionic conductivity

Table 2 Ionic conductivities (σ) of cellulose acetate and conventional Celgard membrane

Sample	Rb, Ω	A, cm^2	t, cm	σ, S/cm
A0W100	39.65	2.835287	0.002943	2.62×10^{-5}
A25W75	8.37	2.835287	0.011367	4.79×10^{-5}
A50W50	77.20	2.835287	0.013433	6.14×10^{-5}
Celgard	936.92	2.835287	0.0025	9.41×10^{-7}

The ionic conductivity calculation shows that a higher acetone composition in CA-based membrane leads to higher ionic conductivity compared to using water only as a non-solvent. Additionally, the results of all CA-based solid polymer electrolyte membranes show better performance than that of Celgard.

4. Conclusions

In conclusion, CA separator membrane was successfully fabricated using the NIPS method with acetone as the solvent and water as the nonsolvent. Higher acetone composition in the coagulation bath facilitated faster phase separation, potentially leading to larger pores, higher electrolyte absorption, lower tensile strength, and lower thermal shrinkage. Increased acetone content also correlated with higher ionic conductivity. The contact angle between CA membrane and water and ethylene glycol decreased with increasing acetone content in the coagulation bath. The wetting ability of the membrane electrolyte increased because of increased membrane porosity. CA-based membranes have shown better mechanical and electrical properties than commercial Celgard membranes. The tensile strength of the pure CA membrane was 6.8 MPa while that of Celgard was 1.42 MPa. The ionic conductivity of the CA membrane with 50% acetone content was 4.79×10^{-4} S/cm while that of Celgard was 9.41×10^{-7} S/cm. These results showed that CA has potential as a viable alternative to replace polyolefin separators.

Acknowledgments

The authors express profound gratitude to the Integrated Laboratory of Advanced Materials Characterization, National Research and Innovation Agency of Indonesia (BRIN), and the Material Research Center, Universitas Indonesia, for the laboratory and materials characterization facility. Special appreciation to the Indonesia Endowment Fund for Education (LPDP) for providing financial support in the PhD program (awardee number 202112210108100).

References

Arrieta, A., Barrera, I., Mendoza, J., 2022. Impedantiometric Behavior of Solid Biopolymer Electrolyte Elaborated from Cassava Starch Synthesized in Different pH. *International Journal of Technology*, Volume 13(4), pp. 912–920

Asghar, M.R., Zhang, Y., Wu, A., Yan, X., Shen, S., Ke, C., Zhang, J., 2018. Preparation of Microporous Cellulose/Poly (Vinylidene Fluoride-Hexafluoropropylene) Membrane for Lithium Ion Batteries by Phase Inversion Method. *Journal of Power Sources*, Volume 379, pp. 197–205

Choi, O., Ingole, P.G., Park, C.H., 2022. Precision-Aiming Tuning of Membranes Prepared by NIPS And Its Performance Enhancement. *Journal of Cleaner Production*, Volume 365, p. 132858

Cui, J., Liu, J., He, C., Li, J., Wu, X., 2017. Composite of Polyvinylidene Fluoride–Cellulose Acetate with $Al(OH)_3$ as a Separator For High-Performance Lithium Ion Battery. *Journal of Membrane Science*, Volume 541, pp. 661–667

Febriasari, A., Suhartini, M., Yunus, A.L., Rahmawati, R., Sudirman, S., Hotimah, B., Hermana, R.F., Kartohardjono, S., Fahira, A. and Permatasari, I.P., 2021. Gamma Irradiation of Cellulose Acetate-Polyethylene Glycol 400 Composite Membrane and Its Performance Test for Gas Separation. *International Journal of Technology*, Volume 12(6), pp. 1198–1206

Jung, J.T., Kim, J.F., Wang, H.H., Di-Nicolo, E., Drioli, E., Lee, Y.M., 2016. Understanding The Non-Solvent Induced Phase Separation (NIPS) Effect During the Fabrication of Microporous PVDF Membranes via Thermally Induced Phase Separation (TIPS). *Journal of Membrane Science*, Volume 514, pp. 250–263

Kahrs, C., Schwellenbach, J., 2020. Membrane Formation via Non-Solvent Induced Phase Separation using Sustainable Solvents: A Comparative Study. *Polymer*, Volume 186, p. 122071

Kartha, T.R., Mallik, B.S., 2020. Revisiting $LiClO_4$ as an Electrolyte for Li-ion Battery: Effect of Aggregation Behavior on Ion-Pairing Dynamics and Conductance. *Journal of Molecular Liquids*, Volume 302, p. 112536

Li, L., Yu, M., Jia, C., Liu, J., Lv, Y., Liu, Y., Zhou, Y., Liu, C., Shao, Z., 2017. Cellulosic Biomass-Reinforced Polyvinylidene Fluoride Separators with Enhanced Dielectric Properties and Thermal Tolerance. *ACS Applied Materials and Interfaces*, Volume 9(24), pp. 20885–20894

Li, Z.H., Zhang, H.P., Zhang, P., Li, G.C., Wu, Y.P., Zhou, X.D., 2008. Effects of the Porous Structure on Conductivity of Nanocomposite Polymer Electrolyte for Lithium Ion Batteries. *Journal of Membrane Science*, Volume 322(2), pp. 416–422

Liang, S., Yan, W., Wu, X., Zhang, Y., Zhu, Y., Wang, H., Wu, Y., 2018. Gel Polymer Electrolytes for Lithium Ion Batteries: Fabrication, Characterization and Performance. *Solid State Ionics*, Volume 318, pp. 2–18

Luiso, S., Williams, A.H., Petrecca, M.J., Roh, S., Velev, O.D. Fedkiw, P.S., 2021. Poly(Vinylidene Difluoride) Soft Dendritic Colloids as Li-Ion Battery Separators. *Journal of The Electrochemical Society*, Volume 168(2), p. 020517

Ngamaroonchote, A., Chotsuwan, C., 2016. Performance and Reliability of Cellulose Acetate-Based Gel Electrolyte for Electrochromic Devices. *Journal of Applied Electrochemistry*, Volume 46(5), pp. 575–582

Pagliero, M., Bottino, A., Comite, A., Costa, C., 2020. Novel Hydrophobic PVDF Membranes Prepared by Nonsolvent Induced Phase Separation for Membrane Distillation. *Journal of Membrane Science*, Volume 596, p. 117575

Ramesh, S., Shanti, R., Morris, E., 2013. Characterization of Conducting Cellulose Acetate Based Polymer Electrolytes Doped With "Green" Ionic Mixture. *Carbohydrate Polymers*, Volume 91(1), pp. 14–21

Razalli, S.M.M., Saaid, S.I.Y.S.M., Ali, A.M.M., Hassan, O.H., Yahya, M.Z.A., 2015. Cellulose Acetate-Lithium Bis (Trifluoromethanesulfonyl) Imide Solid Polymer Electrolyte: ATR-FTIR And Ionic Conductivity Behavior. *Functional Materials Letters*, Volume 8(3), p. 1540017

Rochardjo, H.S.B., Fatkhurrohman, Kusumaatmaja, A., Yudhanto, F., 2021. Fabrication of Nanofiltration Membrane based on Polyvinyl Alcohol Nanofibers Reinforced with Cellulose Nanocrystal using Electrospinning Techniques. *International Journal of Technology*, Volume 12(2), pp. 329–338

Setiaji, D.A., Chalid, M., Abuzairi, T., Efroza, M., Nugraha, A.F., 2022. Effect of Cold Plasma Treatment on Physical Properties of Multilayer Plastics for Polymer Asphalt Applications. *Piston: Journal of Technical Engineering*, Volume 6(1), pp. 1–14

Shi, J., Xia, Y., Yuan, Z., Hu, H., Li, X., Zhang, H., Liu, Z., 2015. Porous Membrane with High Curvature, Three-Dimensional Heat-Resistance Skeleton: A New and Practical Separator Candidate for High Safety Lithium Ion Battery. *Scientific Reports*, Volume 5(1), pp. 1–9

Silva, M.A., Belmonte-Reche, E., Amorim, M.T.P.De., 2021. Morphology and Water Flux of Produced Cellulose Acetate Membranes Reinforced by The Design of Experiments (DOE). *Carbohydrate Polymers*, Volume 254, p. 117407

Song, J., Birbach, N.L., Hinestroza, J.P., 2012. Deposition of Silver Nanoparticles on Cellulosic Fibers via Stabilization of Carboxymethyl Groups. *Cellulose*, Volume 19(2), pp. 411–424

Sudiarti, T., Wahyuningrum, D., Bundjali, B., Arcana, I.M., 2017. Mechanical Strength and Ionic Conductivity of Polymer Electrolyte Membranes Prepared from Cellulose Acetate-Lithium Perchlorate. *In*: IOP Conference Series: Materials Science and Engineering, Volume 223(1), p. 012052

Tabani, Z., Maghsoudi, H., Fathollahi-Zonouz, A., 2021. High Electrochemical Stability of Polyvinylidene Fluoride (PVDF) Porous Membranes Using Phase Inversion Methods For Lithium-Ion Batteries. *Journal of Solid State Electrochemistry*, Volume 25(2), pp. 651–657

Thankamony, R.L., Li, X., Fan, X., Sheng, G., Wang, X., Sun, S., Zhang, X., Lai, Z., 2018. Preparation of Highly Porous Polymer Membranes with Hierarchical Porous Structures via Spinodal Decomposition of Mixed Solvents with UCST Phase Behavior. *ACS Applied Materials and Interfaces*, Volume 10(50), pp. 44041–44049

Wang, H.H., Jung, J.T., Kim, J.F., Kim, S., Drioli, E., Lee, Y.M., 2019. A Novel Green Solvent Alternative for Polymeric Membrane Preparation via Nonsolvent-Induced Phase Separation (NIPS). *Journal of Membrane Science*, Volume 574, pp. 44–54

Xu, R., Huang, X., Lin, X., Cao, J., Yang, J., Lei, C., 2017. The Functional Aqueous Slurry Coated Separator Using Polyvinylidene Fluoride Powder Particles for Lithium-Ion Batteries. *Journal of Electroanalytical Chemistry*, Volume 786, pp. 77–85

Yang, B., Yang, Y., Xu, X., Ke, Y., Pan, Y., Su, L., Wang, Y., Wang, S., Qian, J., Xia, R., Fu, E., 2022. Hierarchical Microstructure and Performance Of PVDF/PMMA/SiO_2lithium Battery Separator Fabricated by Thermally-Induced Phase Separation (TIPS). *Journal of Materials Science*, Volume 57(24), pp. 11274–11288

Zhao, H., Jiang, C., He, X., Ren, J., Wan, C., 2008. Preparation of Micro-Porous Membrane Electrodes and Their Application in Preparing Anodes of Rechargeable Lithium Batteries. *Journal of Membrane Science*, Volume 310(1–2), pp. 1–6